Directed Enzymatic Activation of 1-D DNA Tiles

Sudhanshu Garg,[*,†] Harish Chandran,[†,‡] Nikhil Gopalkrishnan,[†,¶] Thomas H. LaBean,[†,§] and John Reif[†]

Department of Computer Science, Duke University, Durham, NC, USA

E-mail: sgarg@cs.duke.edu

Abstract

The tile assembly model is a Turing universal model of self-assembly where a set of square shaped tiles with programmable sticky sides undergo coordinated self-assembly to form arbitrary shapes, thereby computing arbitrary functions. Activatable tiles are a theoretical extension to the Tile assembly model that enhances its robustness by protecting the sticky sides of tiles until a tile is partially incorporated into a growing assembly. In this paper we experimentally demonstrate a simplified version of the Activatable tile assembly model. In particular, we demonstrate the simultaneous assembly of protected DNA tiles where a set of inert tiles are activated via a DNA polymerase to undergo linear assembly. We then demonstrate step-wise activated assembly where a set of inert tiles are activated sequentially one after another as a result of attachment to a growing 1-D assembly. These are the first experimental demonstrations of enzymatic activation of DNA tiles. We hope that these results will pave way for more sophisticated demonstrations of activated assemblies.

[*]To whom correspondence should be addressed

[†]Department of Computer Science, Duke University, Durham, NC, USA

[‡]Google, Mountain View, CA, USA

[¶]Wyss Institute for Biologically Inspired Engineering, Harvard University, Boston, MA, USA

[§]Department of Materials Science and Engineering, North Carolina State University, Raleigh, NC USA

Keywords

DNA Self Assembly, Polymerase, DNA Tile, Directed, Sequential

DNA Self-Assembly

DNA nanotechnology is a rapidly emerging discipline that uses the molecular recognition properties of DNA to create artificial structures out of DNA. Precise nanoscale objects can be programmatically created using self-assembly of DNA strands and this has resulted in a myriad of nanostructures.[1–10] But more importantly, the dynamic behavior of these DNA nanostructures can also be controlled via the action of other DNA strands[11–17] and enzymes that act on the DNA strands.[18–20]

An important class of DNA nanostructures are tile-based assemblies which are formed via addition of DNA tiles to a growing lattice. The tiles have sticky ends known as pads, which are ssDNA that allow the tile to bind specifically to other tiles having the complementary pads (complementary ssDNA). Winfree *et al.*[1] demonstrated the first lattices self assembled from DNA tiles. Since then many DNA lattices, 2D & 3D, have been demonstrated.[3,5,10] By carefully programming the sticky ends of various tiles, complex lattices can be created.[21,22] Rothemund and Winfree[23] showed in theory that any computable function can be implemented via a set of tiles with carefully designed sticky ends.

Computational Power of 1-D Tile Assembly

Adleman first demonstrated that 1-D self assembly can be used to solve an instance of an intractable problem.[24] Winfree *et al.*[25] proved that linear assembly was equivalent to regular languages, and hence were as powerful as a finite state automaton. Reif[26,27] proposed simple linear tiling self-assemblies for operations such as integer addition, prefix XOR summing of n Boolean bits, string fingerprinting and finite state automata simulations. These were the basis of DNA tiling experiments of Mao *et al.*.[28] These linear tilings were refined by Winfree *et al.*[29] to a class of String Tilings. LaBean *et al.* used these tilings to synthesize a full-adder by using two distinct sets of sticky-ends between adjacent tiles in the assembly to effectively communicate the values of the carry-bits.[30] Linear assemblies have also been a subject of study in theoretical self-assembly.[31] They can be used for making frame tiles,[26] as boundaries,[32] and for arranging nanodots/bioagents in a particular pattern.[33]

Errors in Tile Assembly

Experimental demonstration of complex tilings have been limited by significant assembly errors. Errors in experimental self-assembly have ranged in 1-D from 2-5%,[28] and in 2-D from 10% in 2004,[22] 1.7% in 2007,[34] 0.13% in 2009,[35] 0.05% in 2010,[36] to 0.02% in replicating bits of information.[37]

Theoretical solutions have been suggested to remedy growth errors, facet errors and nucleation errors that arise in DNA tilings.[38–40] A major source of errors are *co-operative growth errors* which occur when a tiles sticky ends match with only some of its neighbours but that is sufficient for it to be wrongly incorporated into the assembly. By making sure that co-operative growth errors (Figure 1) are fixed, a 6-fold increase in error-free assemblies is theoretically possible.[41] Though the trends show a marked decrease in per step assembly errors, final compounded error rates for the global assembly is still high enough to make large scale defect free assemblies infeasible at the moment.

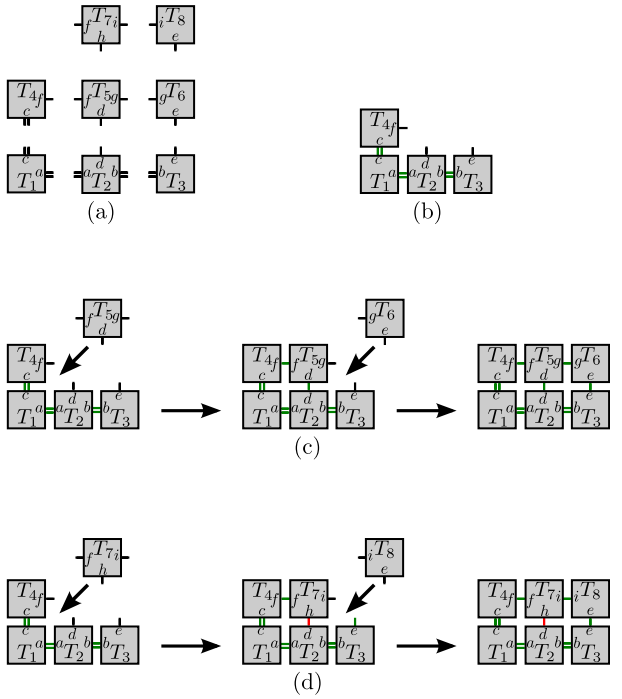

Figure 1: Mechanism of co-operative growth errors. (a) An 8 tile system with a potential for co-operative binding errors in the tile assembly model.[42] Tiles are represented by gray rectangles with face labels. Pad types are shown near the appropriate edge of each tile. Null pads are omitted. Pad strength is indicated by the number of rectangular bars that accompany each pad. Tile system is run at temperature $\tau = 2$. (b) Initial error free assembly of 4 tiles. Correctly matched pads are shaded green. (c) Error free assembly pathway to completion from state (b). (d) Erroneous pathway due to co-operative binding error. Mismatched pad highlighted in red.

Majumder and Reif[43] described a novel protection/deprotection strategy to strictly enforce the direction of tiling assembly growth to ensure the robustness of the assembly process. In their system tiles are initially inactive, meaning that each tile's output sticky ends are protected and cannot bind with other tiles. Only after other tiles bind to the tile's input sticky ends, the tile transitions to an active state and its output sticky ends are exposed, allowing further growth, and the formation of an assembly. In this paper, we demonstrate a 1-D activatable assembly. Though 1-D assemblies do not suf-

fer from co-operative growth errors, they form an ideal system to demonstrate the idea of activated binding sites and serve as the first step in the demonstration of 2D activatable assemblies. We demonstrate the formation of two different 1-D DNA nano-assemblies using activatable tiles. Our first assembly is formed from tiles that are activated simultaneously while our second assembly is formed from tiles that activate sequentially.

1-D Activatable Assemblies

Mechanism 1: Simulatenous Activation of Tiles

In this tile assembly, all the tiles are initially protected via protector strands. (Figure 3) These protector strands inhibit tiles from self-assembling to form the desired final assembly. On introduction of an initiator, the protector strands are removed *simultaneously*, resulting in the activation of the tiles, and subsequent assembly formation.

Mechanism 2: Directed Activation of Tiles

Similar to the previous mechanism, all the tiles are initially protected via protector strands. On the addition of an initiator, an initial set of protected seed tiles are activated. These active tiles can now attach to other protected tiles. Each protected tile that is attached, subsequently gets de-protected (activated). Note that incase an incorrect tile is added to the growing assembly, that growth front of the assembly halts and the assembly does not grow until the incorrect tile detaches and the correct tile diffuses into the correct position.

Comparison of mechanisms

Mechanism 1 is an example of *free self assembly*, while Mechanism 2 is an example of *serial self assembly.*[30] *Serial self assembly* is expected to have lower nucleation errors, since it can initiate only from a seed. *Free self assembly* on the other hand is driven by the spontaenous nucleation of tiles, that takes place when tiles randomly moving around collide into one another. Systems that spontaneously nucleate lose entropy with every tile attachment, resulting in a low average tile-number per assembly. In order to form assemblies with a larger average number of tiles, we have to bias the reaction towards overcoming the entropic loss caused by the additional tiles being added to the assembly. This biasing can be done in two ways, by increasing the length of the sticky ends, or by using enzymatic methods that use an external energy source(s) (dNTPs).

Enzyme-free Activated Tiles: Prior Protected and Layered Tile Mechanisms

Enzyme-free protocols have been suggested by Murata[44] and Fujibayashi *et al.*:[45,46] the Protected Tile Mechanism (PTM) and the Layered Tile Mechanism (LTM) which utilize DNA protecting molecules to form kinetic barriers against spurious assembly. Experimental work using these protocols has been demonstrated.[47] In particular, the authors introduce a protection strand covering the input sticky ends of DNA tiles, and this protection strand is removed only if both inputs correctly match. In the PTM, the output sticky ends are not protected and can bind to a growing assembly before the inputs are deprotected causing an error. In the LTM, the output sticky ends are protected only by 3 nucleotides each and can be easily displaced causing the above-mentioned error. Thus only if we can ensure a deprotection from input to output end, error resilience can be guaranteed. Our activatable tiles technique is a modest step towards this goal.

Design of Activatable Tiling Systems

Mechanism 1: Simultaneous Activation of Tiles

This section describes a prototype experiment to verify the activity of DNA polymerase on a tile system. We demonstrate a 1-D assembly formed from tiles that are all simultaneously activated. Note that this model is not an exact solution to the idea proposed in Majumder

et al.,[43] since the tiles should instead be activated sequentially. This serves as a precursor to our experiments in the next section.

The initial configuration of the system consists of two tile types, both inactive. On the addition of *BST Polymerase*, all instances of both tile types become active, resulting in subsequent assembly formation. This experiment serves as a proof of concept, demonstrating that polymerase can be used as an initiator to activate a set of tiles.

The system consists of two tiles, *Tile A* and *Tile B* each having two sticky ends (pads). Sticky ends are programmed such that the ends of *Tile A* can hybridize to the two sticky ends of *Tile B*. This results in a linear co-polymer of alternating *Tile A*s and *Tile B*s. The tiles themselves are DNA duplexes with overhangs that act as sticky ends. The sticky ends of each tile can be protected via hybridization with a protector complex rendering the tiles inactive. The protector complex contains a primer that can be extended by a strand displacing polymerase which results in deprotection of the tile. This system is illustrated in Figure 3.

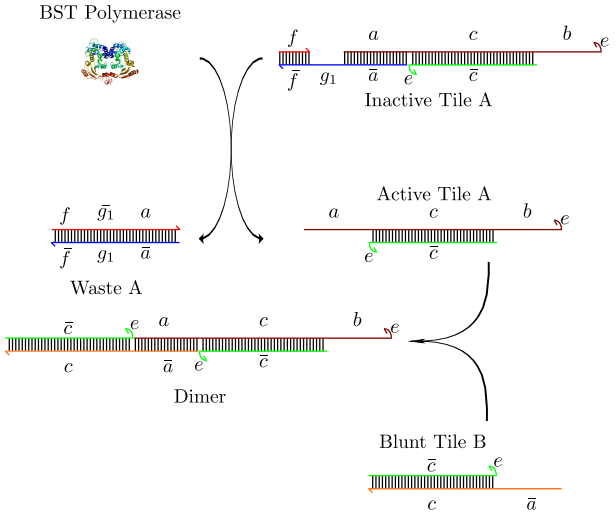

Figure 2: Dimerization of *Tile A* and *Tile B* after Activation: *Inactive Tile A* is transformed into *Active Tile A* by the strand displacing *BST DNA Polymerase*. *Blunt Tile B* is a modified version of *Active Tile B* that lacks the sticky end $\bar{b}$. This prevents the formation of a linear polymer and assembly is halted after a dimer (*Active Tile A* and *Blunt Tile B*) is produced.

The protected versions of *Tile A* and *B*, labeled *Inactive Tile A* and *Inactive Tile B* are synthesized via annealing. *Inactive Tile A* is composed of two parts, *Active Tile A* and *Protector Complex A*. *Active Tile A*, comprised of the strands *acbe* and $\bar{c}e$, is a dsDNA with overhangs. *Protector Complex A* consists of the strand $\bar{a}g_1\bar{f}$ and the primer f. Similarly *Inactive Tile B* is composed of two parts, *Active Tile B* (comprised of the strands $\bar{a}c\bar{b}e$ and $\bar{c}e$) and *Protector Complex B* ($bg_2\bar{f}$ and the *Primer* f). *Inactive Tile A* and *Inactive Tile B* do not react with each other in solution.

In the presence of the strand displacing *BST DNA Polymerase*, the primers on both the inactive tiles are extended to form waste products *Waste A* and *Waste B*. In doing so, the sticky end a of *Inactive Tile A* and sticky end $\bar{b}$ of *Inactive Tile B* are exposed. This activation event results in the formation of *Active Tile A* and *Active Tile B* and they co-polymerize into a linear polymer with alternating A and B tiles. The $3'$ ends of the four DNA strands composing the tiles are augmented with a special domain e, 3 nt (TTT), that is designed to have minimum interaction with any strand in the system. This unhybridized overhang ensures that the polymerase does not spuriously extend these strands.

An additional tile was synthesized by omitting one of the sticky ends in *Tile B*. Specifically, the sticky end $\bar{b}$ of the *Active Tile B* is omitted and this modified tile is labeled *Blunt Tile B*. *Active Tile A*, formed by the activation event described earlier, reacts with *Blunt Tile B* to form a dimer. This process is illustrated in Figure 2, and it serves as an additional experiment demonstrating the formation of a nanoassembly.

Mechanism 2: Directed Activation of Tiles

The scheme depicted in this section activates a tile on binding of the correct input tile (Figure 4). This is in contrast to the one-time switch mechanism of the previous section. Here, an incorrect binding causes the assembly to halt, since the next tile is not activated. The assembly begins with the addition of an initiator (analogous to a *seed tile* in the abstract Tile As-

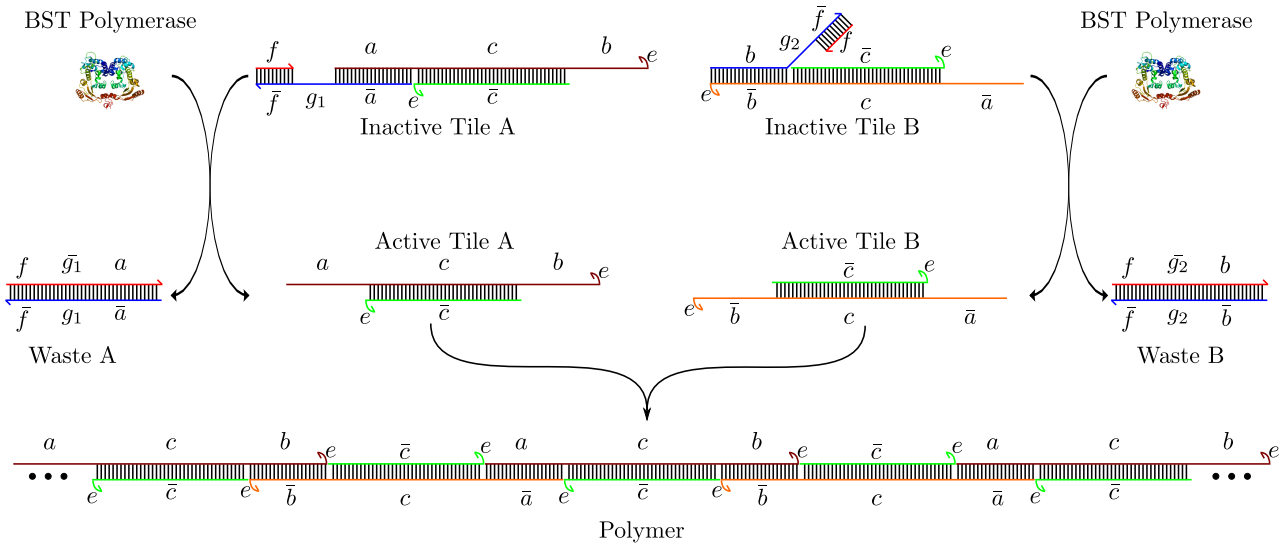

Figure 3: Co-Polymerization of *Tile A* and *Tile B* after Activation: Figure shows two complexes, Inactive *Tile A* composed of four strands: $\bar{c}e$, $\bar{a}g_1\bar{f}$, $acbe$ and f. Inactive *Tile B* composed of 4 strands: $\bar{c}e$, $bg_2\bar{f}$, $\bar{a}c\bar{b}e$ and f. *BST* DNA Polymerase Large Fragment is illustrated by a protein cartoon and does not represent the actual tertiary structure of the enzyme. This strand displacing polymerase extends the prime strand f on both the tiles exposing sticky ends a and $\bar{b}$ in tiles A and B respectively. This transformation of Inactive *Tile A* and Inactive *Tile B* into Active *Tile A* and Active *Tile B* creates waste products Waste A and Waste B respectively. Active *Tile A* and Active *Tile B* now co-polymerizes into a long linear polymer.

sembly Model (aTAM),[42]) that only activates those **instances** of the tiles that have bound to the initiator. These tiles activate subsequent tiles, and the assembly grows at a rate proportional to the reactant concentration.

The system consists of five hairpins, named after their stem domains: *Tiles A, B, C, D* and *E*. Each hairpin has a stem length of 21 nt (chosen to avoid opening of the hairpin at room temperature (RT)), and an unhybridized loop of 42 nt. The stem domains (dsDNA) are initially inactive. Note that overhangs in the hairpins are not needed, serendepitiously removing a common source of leaks.

On addition of the initiator *Seed F*, *Tile A* is activated in the following manner: *Seed F* binds to the hairpin loop of *Tile A*, and the polymerase extends the strand, unravelling the stem domain *a*. Domain *a*, now single stranded, is free to bind to *Tile B*.

The addition of the initiator activates *Tile A*, which can now bind to *Tile B*. *Tile B* in turn activates *Tile C*, *Tile C* activates *Tile D* and *Tile D* activates *Tile E*. The expected end product is shown in Figure 4. This duplex DNA nanostructure is of the form of a DNA ribbon. It has a central seam, which is the ssDNA section of the nanostructure, consisting of spacers. There are dsDNA helices on either end of length 48bp.

Discussions and Conclusions

Simultaneous Activation Mechanism

Leaks in the absence of *BST Polymerase* were seen in both the dimer and polymer mechanisms. The polymer system showed a leak of 14.78% (lane 12, figure 5a)), while the dimer system showed a leak of 11.5% (lane 8, figure 5b)), calculations in supplement section S3.1. In other words, for every 100 tiles of *Inactive Tile A* and *Inactive Tile B*, approximately 15 tiles of *Inactive Tile A* and *Inactive Tile B* leaked to form a polymer over 3 hours. (Similarly 12 tiles of *Inactive Tile A* and *Blunt Tile B* leaked to form a dimer). We attribute this high error rate to the following reasons: 1) Stoichiometry imbalance in formation of tiles - mal-

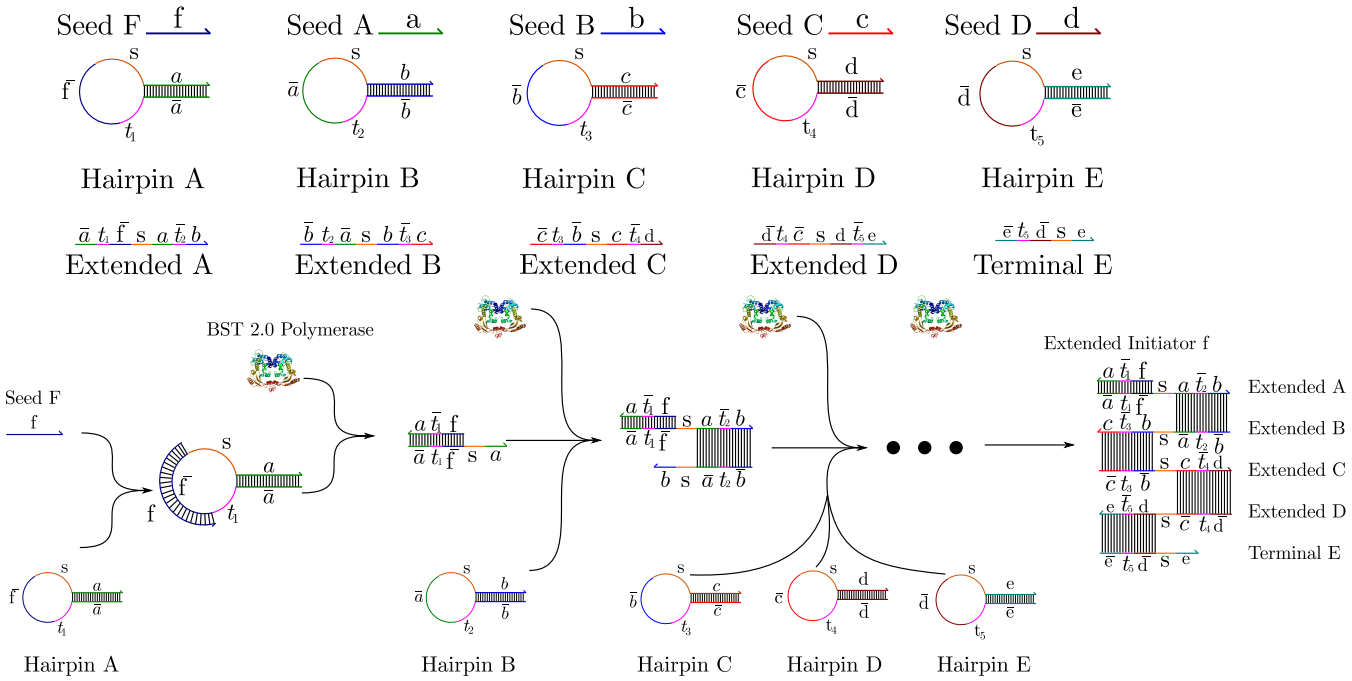

Figure 4: Directed Assembly of Tiles

formed tiles and some tiles without the protector strand can contribute to the leak products observed - this could be fixed by further purification of the tiles post-annealing; 2) There might be a low rate of dissociation at RT of the protector strands ($\bar{a}g_1\bar{f}$ and $bg_2\bar{f}$)that are bound by 16 nt. Increasing this length might help alleviate the leak rates.

Sequential Activation Mechanism

We have achieved directed linear assemblies of sizes 1-5 tiles. Experiments in the presence and absence of polymerase (supplement section S2.1.6) reveal leaks in the system. A leak is defined as the formation of the final tile relative to the quantity of the initial reactants in the absence of a certain initiator (either the polymerase or the seed). In the absence of polymerase (thus presence of initiator), there is no leak (supplement figure S9). This is expected, since there is no polymerase to extend the seed. However, leaks are seen in the presence of polymerase.

Quantitation of the gel fragments shows 45-60% yield for 1 hairpin complexes, ≈30-50% yield for 2-3 hairpin complexes, and ≈20-30% yield for 4-5 hairpin complexes. The leaks account for about 7% of the yield in 2 hairpin systems, 17-27% of the yield in 3 hairpin systems, 14-29% of the yield in 4 hairpin systems, and 25-30% of the yield in 5 hairpin systems. For figure 6, the error rate is 15-18% per tile attachment. We attribute this high error rate to two reasons: 1) impurities in the synthesis of strands; 2) the error rate increases as the number of tiles increases, thus indicating factors such as steric hindrance.

We hypothesize that this method can be scaled up to create larger assemblies. However, the rate of assembly growth might decrease with assembly size because of two reasons: 1) The primer is 21 nt long, and each of the arms of the tiles are 48 bp. For the primer to attach to another hairpin, it will need to be unprotected by the steric hindrances it faces from the other arms. Also, since the primer complement is present in the looped region of the hairpin, it is sterically unstable for the hairpin to move into a position favoured by the primer to attach to. 2) Not unlike the steric hindrance faced by the primer, it is also sterically unfavourable for the polymerase subunit to attach to the 3' end of the primer, and extend another copy of the hairpin, unless there is adequate room for the polymerase to attach (The

size of the BST molecule (PDB ID: 1XWL) is $\approx 7.1 \times 7.8 \times 8.1$nm[48] when visualized by Jmol.[49]) As the length of the assembly increases, the steric hindrances faced in the addition of a new hairpin, and in the involvement of the polymerase increase. We have reduced the steric hindrances by introducing "spacer" domains (denoted by domain *s*, poly-T of 15 nt), which will give room to the the arms of the assembly to accomodate the polymerase and the hairpin motifs. Note the arms of the assembly are analogous to stiff rods, since their lengths lie within the persistence length of DNA. We hypothesize that larger spacer domains will allow scaling of the assembly to larger structures. Another consideration is sequence design, sequences having repeats of 1-4 nt should be avoided when using polymerase (supplement section S4).

Experiments with 0.1 units of polymerase show a significantly reduced yield for higher order hairpins (4 hairpins at 9.75% and 5 hairpins at 8.74% yields, supplement section S2.1.4), and marked streaking in the analytical gels. Thus the quantity of the polymerase influences the expected yield. The use of *BST 2.0 Polymerase* in comparison to *BST Polymerase* also improves the yield of the system (supplement section S2.1.7).

Experiments at a lower concentration of 100nM (supplement section S2.1.8), also resulted in assembly formation, though with a reduced rate. Control experiments with a hairpin missing revealed that the system works as expected, and halts whenever there is a break in the chain (supplement figure S5).

BST polymerase runs optimally at 65^{o}C, while its activity at 37^{o}C is reduced by at least a factor of 2 (supplement figure S8).[50] Since the T_m of these hairpins (70-75^{o}C) is substantially higher than a linear dsDNA of the same length,[51] we utilize the higher processivity of the enzyme, and increase the assembly yield by running the system at a higher temperature 52^{o}C.[52] The leaks were quantified as 6.04% at 50^{o}C, 3.98% at 52^{o}C and 6.45% at 54^{o}C, and thus 52^{o}C was chosen as the default reaction temperature. However, a different temperature might results in better yields. With increasing temperature, the opening rate of a hairpin increases, leading to a higher chance of leak reactions. Increasing the stem length of the hairpins could reduce the opening rate of hairpins at high temperatures, and in turn, leaks. However, due to current limitations in the high error rate of synthesis of strands above 100 nt, our experiments are limited to oligos under 100 nt.

Extensions to 2-D and other Applications

The 1-D sequential assembly system we have described above, has a high error rate of 15-18% in comparison to other enzyme-free 1-D assembly systems 2-5%,[28] 5-10%.[32] However, with large scale improvements in the synthesis of 1) nucleic acid strands and 2) nucleic acid enzymes, we expect the error rates to decrease considerably.

The design we have proposed is currently irreversible. Thus, a tile cannot detach once it has attached to the next tile. However, reversibility is a pre-requisite in a 2-D system, since an incorrect attachment is allowed to detach and re-attach at another location. Future steps would include extending this work to 2-D, and they would require the introduction of reversibility into this system. Beyond their applications to computational tiling, activatable tiles can be used for building sensing and concentration systems, and for reaction catalyzation.[43] The success achieved in engineering such assemblies point to the possibility of more complex activatable systems that can alleviate some of the errors encountered in tile-based DNA self-assembly. They also point to enzymatic methods of self-assembly in addition to the well known non-enzymatic methods of assembling DNA nanostructures.

Materials and Methods

Experiments: Simulatenous Activating Assemblies

This section provides details of the experimental setup and data obtained from the experi-

ments. Post the domain level design of the system, DNA sequences assigned to each domain were designed by hand, taking care to minimize sequence symmetry. The length of the protecting strand $bg_2\bar{f}$ was designed to be greater than the length of the protecting strand $\bar{a}g_1\bar{f}$ to better separate the two complexes in analytical gels. The sequences were validated for any spurious secondary structures via the aid of online DNA folding servers.[53,54] The optimized sequences were obtained at 100 nmol synthesis scale from IDT DNA with standard desalting. DNA strands were PAGE purified and brought up to a working stock concentration of 20 μM. The inactive tile complexes were formed by mixing the constituent strands at an equimolar ratio of 1 μM in 20 μL reaction volume, the only exception being the primer strand f which was added in 2× excess as lower primer concentrations resulted in decreased yield of inactive tiles. The mixture was then heated to 90^o C in a buffer of 1 × TAE with 12.5 mM Mg^{2+} ions and cooled to room temperature (RT $\approx 23^o$ C) over three hours.

1600 units of *BST DNA Polymerase*, Large Fragment at concentration 8000 units/ml were ordered from New England Biolabs. To test the activatable system, 4 pmol each of Inactive *Tile A* and Inactive *Tile B* with 0.1 unit of *BST DNA Polymerase* were incubated in a reaction buffer of 1x Thermopol (20 mM Tris-HCl 10 mM $(NH_4)_2SO_4$, 10 mM KCl, 2 mM $MgSO_4$ and 0.1 % Triton X-100) with 100 μg/ml BSA and 200 μM each of dATP, dCTP, dGTP and dTTP for 3 hours at RT. As a positive control, *Active Tile A* and *Active Tile B* were prepared in separate tubes, post which 4 pmol each was added to 0.1 units of the polymerase and incubated at RT for 3 hours (lane 13, figure 5a). Likewise, 4 pmol each of *Inactive Tile A* and *Inactive Tile B* were incubated in the polymerase reaction buffer in the absence of *BST DNA Polymerase* at RT for 3 hours (negative control, lane 12, figure 5a). In another control experiment, 4 pmol each of the protector complex ($\bar{a}g_1\bar{f} + f$ and $bg_2\bar{f} + f$) were incubated in separate test tubes with *BST DNA Polymerase* in polymerase buffer at RT for 3 hours (lanes 7,9: figure 5a). The complexes were then analyzed in 10 % Non-Denaturing PAGE Gels. The gels and running buffer contain 1 X TAE with 12.5 mM Mg^{2+}. The gels were run for 7 hours at 125 V and then stained and destained using Ethidium Bromide for 45 mins each. Images were obtained using an Alpha Innotech AlphaImager system.

Figure 5a is a non-denaturing PAGE gel image showing the results of these experiments. Lane 14 shows the working of the system where *Inactive Tile A* and *Inactive Tile B* are incubated in polymerase buffer with *BST DNA Polymerase*. We see that the tiles are activated leading to the formation of *Waste A* and *Waste B* and the activated tiles form a linear polymer. Figure 5b is a non-denaturing PAGE gel image showing the results of a similar experiment in the modified system with *Blunt Tile B* resulting in the formation of a dimer.

The experiment above could be performed enzyme-free, by replacing the polymerase with two activating strands $f\bar{g_1}a$ and $\bar{b}\bar{g_2}f$. However, the advantage of using polymerase is that its activity in conjunction with the primer is sequence independent. Hence, a single primer could perform the activation on *both* the strands, as opposed to a need for two distinct activation strands. Also, this could be scaled up to a system containing a larger number of tiles, with a single trigger for activation. The trigger could be the addition of polymerase, or the addition of a single primer in so far as all the protecting strands share the same primer(s).

Experiments: Directed Activating Assemblies

This system consists of five hairpins: A($\bar{a}t_1\bar{f}sa$), B($\bar{b}t_2\bar{a}sb$), C($\bar{c}t_3\bar{b}sc$), D($\bar{d}t_4\bar{c}sd$) and E($\bar{e}t_5\bar{d}se$), that are each 84 nt in length. The sequences Seeds F(f), A(a), B(b), C(c), D(d) each have a single domain 21 nt in length. These domains *f,a,b,c,d,e* are primer domains, that get activated sequentially. The domains $t_1 - t_5$ are 6 nt, while the spacer domain s is a poly-T of 15 nt. These have been included to avoid steric hindrances on primer binding. The persistence length of dsDNA is approximately 50 nm $\approx$ 150bp[55] and the role of the domains

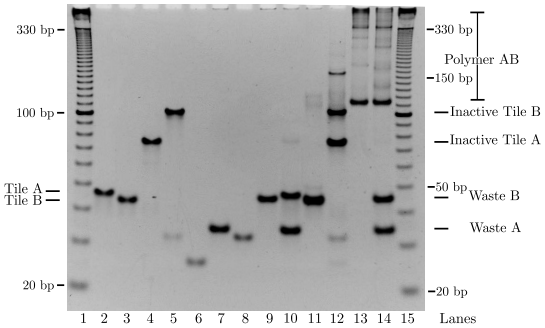

(a) Polymerization of activatable tiles. **Ln 1,15**: 10bp ladder; **Ln 2**: Active Tile A, **Ln 3**: Active Tile B, **Ln 4**: Inactive Tile A, **Ln 5**: Inactive Tile B, **Ln 6**: Primer+ Protector A, **Ln 7**: Primer + Protector A + BST, **Ln 8**: Primer + Protector B, **Ln 9**: Primer + Protector B + BST, **Ln 10**: Inactive Tile A + BST, **Ln 11**: Inactive Tile B + BST, **Ln 12**: Inactive Tile A + Inactive Tile B, **Ln 13**: Active Tile A + Active Tile B, **Ln 14**: Inactive Tile A + Inactive Tile B + BST.

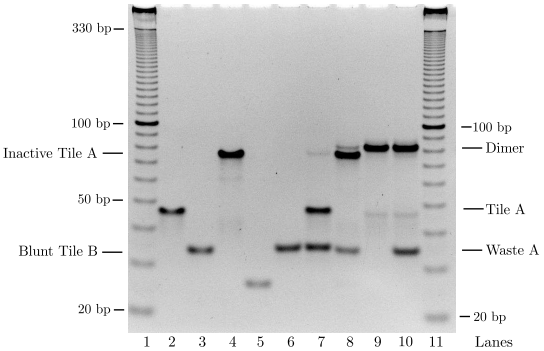

(b) Dimer Formation. **Ln 1,11**: 10bp ladder; **Ln 2**: Active Tile A, **Ln 3**: Blunt Tile B, **Ln 4**: Inactive Tile A, **Ln 5**: Primer+ Protector A, **Ln 6**: Primer + Protector A + BST, **Ln 7**: Inactive Tile A + BST, **Ln 8**: Inactive Tile A + Blunt Tile B, **Ln 9**: Active Tile A + Blunt Tile B, **Ln 10**: Inactive Tile A + Blunt Tile B + BST.

Figure 5: Formation of Dimer and Polymers

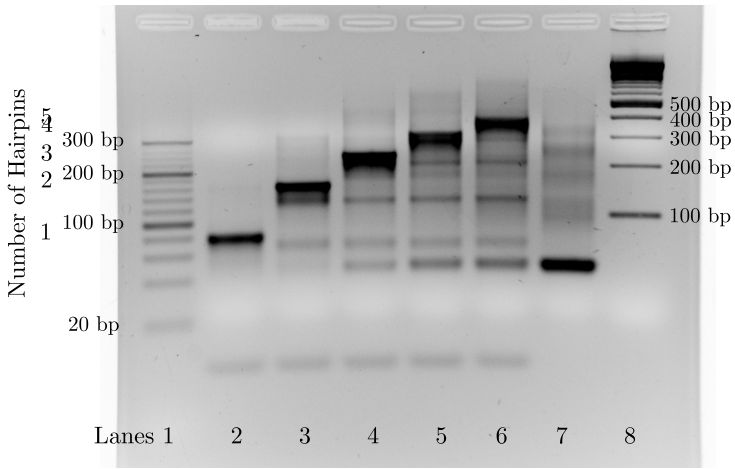

(a) **Ln 1:** 20 bp ladder, **Ln 2:** Hairpin A + Seed F (0.5uM), **Ln 3:** Hairpins A+B + Seed F (0.5uM), **Ln 4:** Hairpins A+B+C + Seed F (0.5uM), **Ln 5:** Hairpins A+B+C+D + Seed F (0.5uM), **Ln 6:** Hairpins A+B+C+D+E + Seed F (0.5uM), **Ln 7:** (Leak) Hairpins A+B+C+D+E (0.5uM), **Ln 8:** 2-log ladder

Lane	Yield
2	**33.33%**
3	**27.33%**
4	**31.33%**
5	**19.33%**
6	**16%**
7 (leak)	**4%**

Figure 6: Sequential assembly using BST Polymerase at 52^{o}C.

$t_1 - t_5$ is to increase the size of the hairpin loop so that the binding of the primer to the loop does not result in molecular beacon like activity, initiating a leak reaction.

The hairpins were created in 5 μM aliquots, and were "quick-annealed", by heating to 90^0C(5 mins) and cooled at RT(5 mins). 1600 units of *BST 2.0 DNA Polymerase* at concentration 8000 units/ml were ordered from New England Biolabs. 2 μl of each hairpin (10 pmol), 4 μl of the seed (20 pmol, at 2x concentration to ensure all reactions proceed to completion), and 2 units of *BST 2.0 DNA Polymerase* were incubated in a reaction buffer of 1X Isothermal Amplification Buffer (20 mM Tris-HCl, 10 mM $(NH_4)_2SO_4$, 50 mM KCl, 2 mM $MgSO_4$ and 0.1 % Tween® 20) with 100 μg/ml BSA and 1 mM each of dATP, dCTP, dGTP and dTTP for 1 hour at 52^{o}C. The hairpins were mixed stoichiometrically to achieve a final concentration of 0.5 μM (Seed 1μM) in a total reaction volume of 20ul. 10 μl of Mineral Oil (M5904 Sigma, density 0.84g/ml) was added to the total reaction mixture pre-incubation, to prevent evaporation. 4 μl of 6X Native Dye (0.25% Bromophenol Blue, 0.25% Xylene Cyanol, 12.5mM TAE/Mg^{2+}, 50% Glycerol) was added post-incubation, and 3.6 μl (1.5 pmol) of the complexes were analyzed in 3% native agarose gels (5mm thick, 27 ml, prepared for use in LB Buffer (Faster Better Media, LLC). The agarose gels were pre-run empty for 2 mins, and then run with samples for 20 mins at 250 V (in an ice bath to prevent smiley gel bands). Images were obtained using an Alpha Innotech AlphaImager system. The results of the experiments can be seen in Figure 6. Stepwise reactions have been performed to verify the activity of one, two, three, four and five hairpins, each step involving a single seed and DNA polymerase (supplement section S2.1). Reactions are performed at 52^{o}C (and 37^{o}C; supplement section S2.1.5), lower than the T_m of each tile (70-75^{o}C). Negative control experiments involving only the hairpins (with/without polymerase and/or primer), reveal 0-20% leaks in the system. The leaks however, vary with temperature (supplement section S2.1.4).

Acknowledgement The authors thank Tianqi Song, Hieu Bui, Reem Mokhtar and the anonymous referees, for their valuable suggestions and critiques on the article. This work was supported in parts by NSF CCF-1217457, NSF CCF-1141847 and NSF EMT Grant CCF-0829798.

Supporting Information Available: DNA Sequence Design and control experiments. This material is available free of charge via the Internet at `http://pubs.acs.org/`.

References

1. Winfree, E.; Liu, F.; Wenzler, L.; Seeman, N. Design and Self-assembly of Two-dimensional DNA Crystals. *Nature* **1998**, *394*, 539–544.

2. LaBean, T.; Yan, H.; Kopatsch, J.; Liu, F.; Winfree, E.; Reif, J.; Seeman, N. Construction, Analysis, Ligation, and Self-Assembly of DNA Triple Crossover Complexes. *Journal of the American Chemical Society* **2000**, *122*, 1848–1860.

3. Yan, H.; Park, S. H.; Finkelstein, G.; Reif, J.; LaBean, T. DNA-Templated Self-Assembly of Protein Arrays and Highly Conductive Nanowires. *Science* **2003**, *301*, 1882–1884.

4. Shih, W.; Quispe, J.; Joyce, G. A 1.7-kilobase Single-stranded DNA that Folds into a Nanoscale Octahedron. *Nature* **2004**, *427*, 618–621.

5. He, Y.; Chen, Y.; Liu, H.; Ribbe, A.; Mao, C. Self-Assembly of Hexagonal DNA Two-Dimensional (2D) Arrays. *Journal of the American Chemical Society* **2005**, *127*, 12202–12203.

6. Rothemund, P. Folding DNA to Create Nanoscale Shapes and Patterns. *Nature* **2006**, *440*, 297–302.

7. He, Y.; Ye, T.; Su, M.; Zhang, C.; Ribbe, A.; Jiang, W.; Mao, C. Hierarchical Self-assembly of DNA into Symmetric

Supramolecular Polyhedra. *Nature* **2008**, *452*, 198–201.

8. Douglas, S.; Dietz, H.; Liedl, T.; Hogberg, B.; Graf, F.; Shih, W. Self-assembly of DNA into Nanoscale Three-dimensional Shapes. *Nature* **2009**, *459*, 414–418.

9. Dietz, H.; Douglas, S.; Shih, W. Folding DNA into Twisted and Curved Nanoscale Shapes. *Science* **2009**, *325*, 725–730.

10. Zheng, J.; Birktoft, J.; Chen, Y.; Wang, T.; Sha, R.; Constantinou, P.; Ginell, S.; Mao, C.; Seeman, N. From Molecular to Macroscopic via the Rational Design of a Self-assembled 3D DNA Crystal. *Nature* **2009**, *461*, 74–78.

11. Yurke, B.; Turberfield, A.; Mills, A.; Simmel, F.; Neumann, J. A DNA-fuelled Molecular Machine Made of DNA. *Nature* **2000**, *406*, 605–608.

12. Sherman, W.; Seeman, N. A Precisely Controlled DNA Biped Walking Device. *Nano Letters* **2004**, *4*, 1203–1207.

13. Shin, J.-S.; Pierce, N. A Synthetic DNA Walker for Molecular Transport. *Journal of American Chemical Society* **2004**, *126*, 10834–10835.

14. Tian, Y.; Mao, C. Molecular Gears: A Pair of DNA Circles Continuously Rolls against Each Other. *Journal of American Chemical Society* **2004**, *126*, 11410–11411.

15. Yin, P.; Choi, H.; Calvert, C.; Pierce, N. Programming Biomolecular Self-assembly Pathways. *Nature* **2008**, *451*, 318–322.

16. Green, S.; Bath, J.; Turberfield, A. Coordinated Chemomechanical Cycles: A Mechanism for Autonomous Molecular Motion. *Physical Review Letters* **2008**, *101*.

17. Venkataraman, S.; Dirks, R.; Rothemund, P.; Winfree, E.; Pierce, N. An Autonomous Polymerization Motor Powered by DNA Hybridization. *Nature Nanotechnology* **2007**, *2*, 490–494.

18. Yin, P.; Yan, H.; Daniell, X.; Turberfield, A.; Reif, J. A Unidirectional DNA Walker Moving Autonomously Along a Linear Track. *Angewandte Chemie International Edition* **2004**, *116*, 5014–5019.

19. Bath, J.; Green, S.; Turberfield, A. A Free-Running DNA Motor Powered by a Nicking Enzyme. *Angewandte Chemie International Edition* **2005**, *44*, 4358–4361.

20. Sahu, S.; LaBean, T.; Reif, J. A DNA Nanotransport Device Powered by Polymerase ϕ29. *Nano Letters* **2008**, *8*, 3870–3878.

21. Park, S. H.; Pistol, C.; Ahn, S. J.; Reif, J.; Lebeck, A.; LaBean, C. D. T. Finite-Size, Fully Addressable DNA Tile Lattices Formed by Hierarchical Assembly Procedures. *Angewandte Chemie International Edition* **2006**, *45*, 735–739.

22. Rothemund, P.; Papadakis, N.; Winfree, E. Algorithmic Self-Assembly of DNA Sierpinski Triangles. *PLoS Biology* **2004**, *2*, 424–436.

23. Rothemund, P.; Winfree, E. The Program-Size Complexity of Self-Assembled Squares. *Symposium on Theory of Computing* **2000**, 459–468.

24. Adleman, L. Molecular Computation of Solutions to Combinatorial Problems. *Science* **1994**, *266*, 1021–1024.

25. Winfree, E.; Yang, X.; Seeman, N. Universal Computation via Self-assembly of DNA: Some Theory and Experiments. *DNA Based Computers II, DIMACS* **1996**, *44*, 191–213.

26. Reif, J. Local Parallel Biomolecular Computation. *DNA-Based Computers, III* **1997**, 217–254.

27. Reif, J. H.; LaBean, T. H.; Sahu, S.; Yan, H.; Yin, P. Molecular Computations Using Self-Assembled DNA Nanostructures and Autonomous Motors. *Unconventional Programming Paradigms* **2004**, 14.

28. Mao, C.; Labean, T.; Reif, J.; Seeman, N. Logical Computation Using Algorithmic Self-assembly of DNA Triple-crossover Molecules. *Nature* **2000**, *407*, 493–496.

29. Winfree, E.; Eng, T.; Rozenberg, G. String Tile Models for DNA Computing by Self-Assembly. *DNA Computing* **2000**, 63–88.

30. LaBean, T.; Winfree, E.; Reif, J. Experimental Progress in Computation by Self-Assembly of DNA Tilings. *DNA Based Computers V, DIMACS* **1999**,

31. Chandran, H.; Gopalkrishnan, N.; Reif, J. The Tile Complexity of Linear Assemblies. *International Colloquium on Automata, Languages and Programming* **2009**, 235–253.

32. Schulman, R.; Lee, S.; Papadakis, N.; Winfree, E. One Dimensional Boundaries for DNA Tile Self-Assembly. *DNA Computing* **2003**, 108–126.

33. Demaine, E.; Eisenstat, S.; Ishaque, M.; Winslow, A. In *DNA Computing and Molecular Programming*; Cardelli, L., Shih, W., Eds.; Lecture Notes in Computer Science; Springer Berlin Heidelberg, 2011; Vol. 6937; pp 100–114.

34. Fujibayashi, K.; Hariadi, R.; Park, S. H.; Winfree, E.; Murata, S. Toward Reliable Algorithmic Self-Assembly of DNA Tiles: A Fixed-Width Cellular Automaton Pattern. *Nano Letters* **2008**, *8*, 1791–1797, PMID: 18162000.

35. Barish, R. D.; Schulman, R.; Rothemund, P. W. K.; Winfree, E. An Information-bearing Seed for Nucleating Algorithmic Self-assembly. *Proceedings of the National Academy of Sciences* **2009**, *106*, 6054–6059.

36. Chen, H.-L.; Doty, D. Parallelism and Time in Hierarchical Self-assembly. Proceedings of the Twenty-third Annual ACM-SIAM Symposium on Discrete Algorithms. 2012; pp 1163–1182.

37. Schulman, R.; Yurke, B.; Winfree, E. Robust self-replication of combinatorial information via crystal growth and scission. *Proceedings of the National Academy of Sciences* **2012**,

38. Winfree, E.; Bekbolatov, R. Proofreading Tile Sets: Error Correction for Algorithmic Self-Assembly. *DNA Computing* **2003**, 126–144.

39. Chen, H.-L.; Goel, A. Error Free Self-assembly Using Error Prone Tiles. *DNA Computing* **2004**, 62–75.

40. Reif, J.; Sahu, S.; Yin, P. Compact Error-Resilient Computational DNA Tiling Assemblies. *DNA Computing* **2004**, 293–307.

41. Rothemund, P. W. K. Using lateral capillary forces to compute by self-assembly. *Proceedings of the National Academy of Sciences* **2000**, *97*, 984–989.

42. Winfree, E. Algorithmic Self-Assembly of DNA. Ph.D. thesis, California Institute of Technology, 1998.

43. Majumder, U.; LaBean, T.; Reif, J. Activatable Tiles: Compact, Robust Programmable Assembly and Other Applications. *DNA Computing* **2007**,

44. Murata, S. Self-assembling DNA tiles - mechanisms of error suppression. SICE 2004 Annual Conference. 2004; pp 2764–2767 vol. 3.

45. Fujibayashi, K.; Murata, S. A Method of Error Suppression for Self-assembling DNA Tiles. *DNA Computing* **2005**, *3384*, 113–127.

46. Fujibayashi, K.; Zhang, D. Y.; Winfree, E.; Murata, S. Error suppression mechanisms for DNA tile self-assembly and their simulation. **2009**, *8*, 589–612.

47. Zhang, D. Y.; Hariadi, R. F.; Choi, H. M.; Winfree, E. Integrating DNA strand-displacement circuitry with DNA tile self-assembly. *Nat Commun* **2013**, *4*.

48. Kiefer, J. R.; Mao, C.; Hansen, C. J.; Basehore, S. L.; Hogrefe, H. H.; Braman, J. C.; Beese, L. S. Crystal structure of a thermostable Bacillus {DNA} polymerase l large fragment at 2.1 resolution. *Structure* **1997**, *5*, 95 – 108.

49. Hanson, R. M.; Prilusky, J.; Renjian, Z.; Nakane, T.; Sussman, J. L. JSmol and the Next-Generation Web-Based Representation of 3D Molecular Structure as Applied to Proteopedia. *Israel Journal of Chemistry* **2013**, *53*, 207–216.

50. Stenesh, J.; Roe, B. {DNA} polymerase from mesophilic and thermophilic bacteria: I. Purification and properties of {DNA} polymerase from Bacillus licheniformis and Bacillus stearothermophilus. *Biochimica et Biophysica Acta (BBA) - Nucleic Acids and Protein Synthesis* **1972**, *272*, 156 – 166.

51. Paner, T. M.; Amaratunga, M.; Doktycz, M. J.; Benight, A. S. Analysis of melting transitions of the DNA hairpins formed from the oligomer sequences d[GGATAC(X)4GTATCC] (X = A, T, G, C). *Biopolymers* **1990**, *29*, 1715–1734.

52. Notomi, T.; Okayama, H.; Masubuchi, H.; Yonekawa, T.; Watanabe, K.; Amino, N.; Hase, T. Loop-mediated isothermal amplification of DNA. *Nucleic Acids Research* **2000**, *28*, e63.

53. Zuker, M. MFOLD Web Server for Nucleic Acid Folding and Hybridization Prediction. *Nucleic Acids Research* **2003**, *31*, 3406–3415.

54. Zadeh, J.; Steenberg, C.; Bois, J.; Wolfe, B.; Pierce, M.; Khan, A.; Dirks, R.; Pierce, N. NUPACK: Analysis and Design of Nucleic Acid Systems. *Journal of Computational Chemistry* **2010**, *32*, 170–173.

55. Hays, J. B.; Magar, M. E.; Zimm, B. H. Persistence length of DNA. *Biopolymers* **1969**, *8*, 531–536.

Graphical TOC Entry